

Resonances in Ferromagnetic Gratings Detected by Microwave Photoconductivity

Y. S. Gui, S. Holland, N. Mecking, and C.-M. Hu*

Institut für Angewandte Physik und Zentrum für Mikrostrukturforschung, Universität Hamburg, Jungiusstraße 11, 20355 Hamburg, Germany

(Received 18 February 2005; published 28 July 2005)

We investigate the impact of microwave excited spin excitations on the dc charge transport in a ferromagnetic (FM) grating. We observe both resonant and nonresonant microwave photoresistance, which are caused, respectively, by spin and charge dissipations of the microwave power into the FM. A macroscopic model based on Maxwell and Landau-Lifschitz equations reveals the mixing of spin and charge dissipations, which shows that the ferromagnetic antiresonance is shifted when the conductivity is anisotropic. We find that the microwave photoconductivity provides a powerful new tool to study the interplay between photonic, spintronic, and charge effects in FM microstructures.

DOI: [10.1103/PhysRevLett.95.056807](https://doi.org/10.1103/PhysRevLett.95.056807)

PACS numbers: 73.50.Pz, 41.20.Jb, 42.79.Dj, 76.50.+g

The connection between the dc and high frequency response of the metal to external fields looks like a one-way path. On the one hand, it is textbook knowledge that due to the eddy current dissipation, the dc conductivity σ_0 determines the skin depth $\delta = \sqrt{2/\mu_0\sigma_0\omega}$ of the electromagnetic radiation with the frequency $\omega = 2\pi f$, where μ_0 is the permeability of vacuum. On the other hand, there is little knowledge about the inverse effect of the high frequency response on the dc transport in metals, which is in contrast to the case of semiconductors, where a whole zoo of photoconductivity phenomena, ranging from the intrinsic, extrinsic, to the bolometric effect, are all based on such an influence.

Recently, a breakthrough has been achieved in ferromagnetic (FM) metallic multilayers. By combining the giant magnetoresistance effect with the microwave absorption, high frequency resonances were detected by measuring the dc resistance [1]. This experiment bridged static and dynamic properties of FM multilayers, and paved the way for recent highlights of generating microwave oscillations by a spin-polarized dc current [2]. Despite broad interest in studying the interplay of magnetostatics and magnetodynamics, the basic question of the impact of the high frequency response on the dc transport in a single layer FM metal remains open.

In this Letter, we answer this question by performing microwave photoconductivity measurements directly on a single layer FM microstrip. Our primary aim is to explore the bolometric effect [3,4] in the FM metal, which may bridge the high frequency absorbance $A(\omega)$ with the dc resistance change ΔR via a simple relation

$$\Delta R = SA(\omega), \quad (1)$$

where $S = \frac{\partial R}{\partial T} \frac{P_0 \tau_e}{C_e}$ is a sensitivity parameter that depends on the specific heat C_e of electrons, the incident power P_0 of the radiation, and the energy relaxation time τ_e of photoexcited charges. The relation was previously only known for semiconductors [4]. We demonstrate that based on the interplay between spin dynamics, charge transport,

and microwave absorptions, both resonant spin excitations such as the ferromagnetic resonance (FMR) [5] and non-resonant eddy current dissipation can be detected by the photoconductivity technique. Using a model based on Maxwell and Landau-Lifschitz equations, we reveal the unique nature of the mixing of spin and charge dynamic response, which causes a characteristic conductivity-induced shift of the ferromagnetic antiresonance (FMAR) [6].

Our experiments are performed on an array of $\text{Ni}_{80}\text{Fe}_{20}$ (Permalloy, Py) microstrip with a width $W = 50 \mu\text{m}$ and a thickness $d = 60 \text{ nm}$. As illustrated in the insets of Fig. 1, the strip has a total length $L \approx 10 \text{ cm}$ and runs meandering in a square of about $3 \times 3 \text{ mm}^2$, forming 30 periods of FM grating with a period $a = 70 \mu\text{m}$. The Py strip is deposited

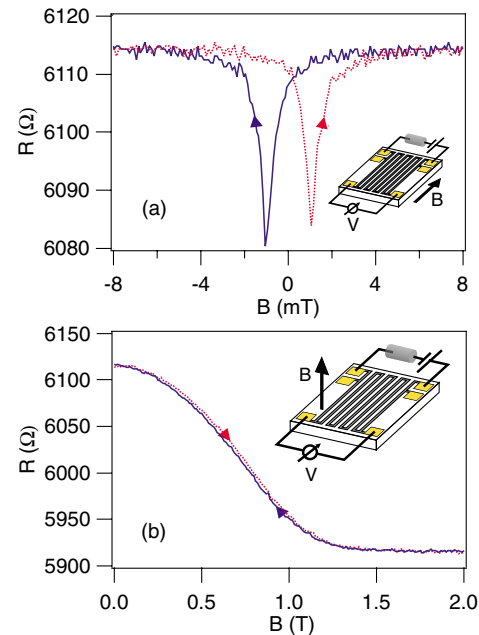


FIG. 1 (color online). (a) Parallel ($\theta = 0^\circ$) and (b) perpendicular ($\theta = 90^\circ$) AMR effect measured with the applied magnetic-field and current bias as shown in the inset.

on a semi-insulating GaAs substrate using photolithography and lift-off techniques. The dc conductivity σ_0 of the Py strip is determined to be $3.2(5.0) \times 10^4 \Omega^{-1} \text{cm}^{-1}$ at 300 (4.2) K. A swept-signal generator is connected to a circular waveguide with a diameter of about 1 cm, which brings unpolarized microwave radiations with f between 17.5–20 GHz down to the sample set in a cryostat. Because the wavelength of the imposed microwave ($\lambda \approx 1.5$ cm) is much larger than the period of the grating, the conductivity of our sample is macroscopically anisotropic for the dynamic response.

Before discussing the photoconductivity of the Py strip, we show in Fig. 1 the static property of our sample without microwave radiations. By applying the external magnetic field $H = B/\mu_0$ along the easy axis parallel ($\theta = 0^\circ$) to the current flow in the strip, we measure the anisotropic magnetoresistance (AMR) and plot it [7] in Fig. 1(a). The sharp minimum at ± 1.2 mT corresponds to the coercive field of the strip [8], which increases with increasing the angle θ (not shown). At $\theta = 90^\circ$ when the applied B field is along the hard axis perpendicular to the strip plane, perpendicular AMR is measured and plotted in Fig. 1(b). The estimated saturation magnetization (M_0) is about 1.2 T/ μ_0 and the normalized AMR is about 3.2%, both in agreement with earlier reports [8].

We perform the photoconductivity experiment at $\theta = 90^\circ$ in the Faraday configuration with the microwave wave vector $\mathbf{k} \parallel \mathbf{B}$. Figure 2 shows typical photoresistance traces measured as a function of the B field at 4.2 K for different microwave frequencies. Data measured at high temperatures show similar features. The curves are verti-

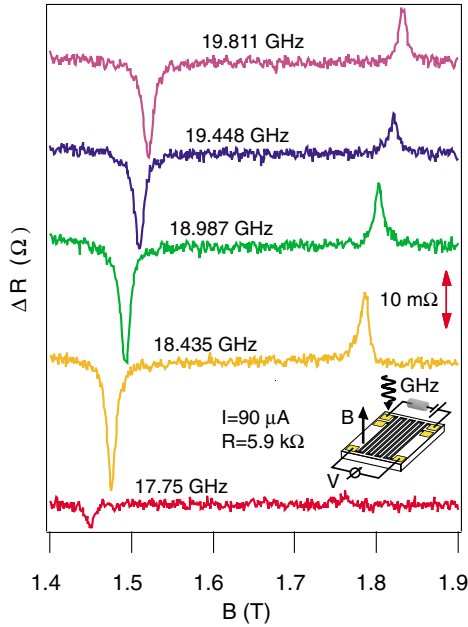


FIG. 2 (color online). Microwave photoresistance (vertically offset for clarity) of the Py strip measured as a function of the magnetic field at 4.2 K and at different microwave frequencies. The inset shows the measurement configuration.

cally offset for clarity. A dc current of $I = 90 \mu\text{A}$ is applied. The radiation-induced voltage change ΔV is measured via lock-in technique by modulating the microwave power with a frequency of 123 Hz. The photoresistance $\Delta R = \Delta V/I$ measures the microwave-induced dc magnetoresistance change of the Py strip. In addition to a non-resonant background photoresistance at the order of 10 m Ω , which is about a few ppm of the dc magnetoresistance R of the Py strip, we observe clearly two resonances. One appears as a peak and the other as a dip. The resonant field for both shifts with f . We find that ΔR increases with increasing power. The data shown in Fig. 2 are measured by setting the output power of the swept-signal generator at 24 dbm, however, the power that reaches the sample via the long waveguide is significantly reduced. At 17.75 GHz, when f approaches the cutoff frequency of the waveguide, ΔR is obviously reduced.

To shed light onto the observed photoconductivity effect, we begin by analyzing the magnetodynamic response function of our sample. The dynamic susceptibility tensor $\hat{\chi}$, which links the dynamic magnetization \mathbf{m} and the dynamic magnetic field \mathbf{h} via $\mathbf{m} = \hat{\chi} \cdot \mathbf{h}$, can be obtained by solving the Landau-Lifschitz equation [9]. For simplicity, we restrict our analysis to the field range of $H > M_0$ where resonances are observed. Since in our sample $d \ll L, W$, we start by treating it as a 2D film, taking into account the demagnetization field but neglecting the anisotropy and the exchange field. We get the dynamic permeability tensor

$$\hat{\mu} = \hat{1} + \hat{\chi} = \begin{pmatrix} \mu_L & \mu_T & 0 \\ -\mu_T & \mu_L & 0 \\ 0 & 0 & 1 \end{pmatrix}$$

with the longitudinal (μ_L) and transversal (μ_T) complex permeability given by

$$\mu_L = 1 + \frac{\omega_M(\omega_r - i\alpha\omega)}{(\omega_r - i\alpha\omega)^2 - \omega^2}, \quad (2)$$

$$\mu_T = \frac{i\omega_M\omega}{(\omega_r - i\alpha\omega)^2 - \omega^2}.$$

Here, α is the dimensionless Gilbert damping parameter. We define $\omega_M = \gamma M_0$ and $\omega_r = \gamma(H - M_0)$, with $\gamma = g\mu_B\mu_0/\hbar$ the gyromagnetic ratio which depends on the g factor and the Bohr magneton μ_B .

The dynamic permeability tensor $\hat{\mu}$ describes the gyro-tropic response of the FM metal. In the Faraday configuration, its eigenvalues can be found by solving the equation $\mathbf{k}(\mathbf{k} \cdot \mathbf{h}) + (k_0^2 \epsilon \hat{\mu} - \mathbf{k}^2)\mathbf{h} = 0$ deduced from the Maxwell equations [10] with $\mathbf{h} \propto \exp(i\mathbf{k} \cdot \mathbf{r} - i\omega t)$. We obtain

$$\mu_{\pm} = \mu_L \mp i\mu_T = \frac{\omega_r + \omega_M \mp \omega - i\alpha\omega}{\omega_r \mp \omega - i\alpha\omega}, \quad (3)$$

which define two circular polarized electromagnetic eigenmodes propagating in the FM film whose wave vectors are given by $k_{\pm}^2 = \epsilon\mu_{\pm}k_0^2$. Here $\epsilon \approx i\sigma_0/\epsilon_0\omega$ is the complex permittivity of the FM film, ϵ_0 , c , and $k_0 = \omega/c$ are the

permittivity, the velocity, and the wave vector of light in vacuum. The k_+ mode results from the coupling of the right circular electromagnetic wave with the magnetization, which excites the FMR at the resonant frequency ω_r .

In Fig. 3(a), we plot the magnetic-field dispersion of the peak (solid square) and dip (open circle) measured from photoconductivity spectra. By fitting the dispersion of the peak using the relation $\omega_r = \gamma(H - M_0)$, we obtain $\gamma = 183\mu_0$ GHz/T (corresponding to $g = 2.08$) which agrees well with the published values [11], and $M_0 = 1.15$ T/ μ_0 , which is consistent with the value (1.2 T/ μ_0) estimated from the AMR effect. Therefore, we identify the resonant peak of the photoresistance as the FMR, which has the microscopic origin of Larmor precession of spins in the FM metal [5].

With fitted values for γ and M_0 , we calculate and plot in Fig. 3(b) the B -field dependence of μ_+ for $\omega/2\pi = 35$ GHz. From a line shape fit that we will describe later, we take $\alpha = 0.0075$. The real part of μ_+ has two zeros. At the zero indicated by the upward arrow located at $\omega = \omega_r = \gamma(H - M_0)$, $\text{Im}(\mu_+)$ shows a pole, which corresponds to the macroscopic condition of resonantly enhanced absorption due to the FMR. For $H > M_0$, μ_- has neither pole nor zero (not shown), because the FMR is inactive to the left circular polarized electromagnetic wave.

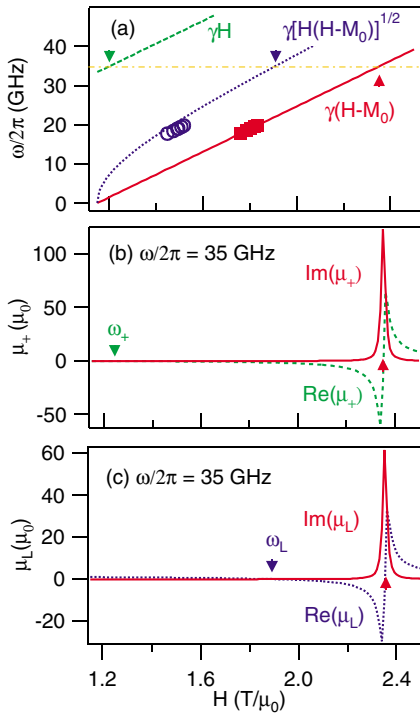


FIG. 3 (color online). (a) Measured peak positions (solid square) are fitted to the FMR dispersion (solid line). Measured dip positions (open circle) are compared with FMAR dispersions calculated using μ_+ (dashed line) and μ_L (dotted curve). (b) μ_+ and (c) μ_L are calculated at $\omega/2\pi = 35$ GHz, using parameters $M_0 = 1.15$ T/ μ_0 , $\alpha = 0.0075$, and $\gamma = 183\mu_0$ GHz/T. Arrows indicate the condition for $\text{Re}(\mu) = 0$.

Note that there is a second zero for $\text{Re}(\mu_+)$ located at $\omega = \omega_+ = \gamma H$, which is indicated by the downward arrow in Fig. 3(b). At this condition, $\text{Im}(\mu_+)$ is also nearly zero, hence the dynamic susceptibility $\chi_+ \approx -1$. This is the resonant condition for the FMAR of FM films at which the eddy current dissipation is suppressed. Early microwave transmission experiments have confirmed enhanced transmission and reduced absorption at the FMAR [6]. One would therefore attribute the resonant photoresistance dip in Fig. 2 to the FMAR. However, as shown in Fig. 3(a), measured dip positions (open circles) lie far away from the dashed line plotted for the relation $\omega_+ = \gamma H$.

Now we go to the next step to model the anisotropic conductivity of our grating. We use a simple approximation treating the grating as a linear polarizer [12,13] with a macroscopic permittivity tensor

$$\hat{\epsilon} = \begin{pmatrix} 1 & 0 & 0 \\ 0 & \epsilon & 0 \\ 0 & 0 & 1 \end{pmatrix},$$

neglecting its microscopic geometric details. By using $\hat{\epsilon}$ instead of ϵ in Maxwell equations, we find that the eigenmode propagating in the FM grating is nearly linear polarized with the wave vector given by $k_L^2 \approx \epsilon \mu_L k_0^2$. The behavior of μ_L plotted in Fig. 3(c) is similar to that of μ_+ near the FMR, but shows a characteristic difference for the FMAR. From $\text{Re}(\mu_L) = 0$, we get $\omega_L = \gamma\sqrt{H(H - M_0)}$ for the FMAR, which we plot in Fig. 3(a) as the dotted curve.

With μ_L given in Eq. (2), we go a step further to calculate the absorbance $A(\omega)$ of the Py grating on top of an insulating GaAs substrate, using a procedure similar to that we derived recently for a semiconductor multilayer system [14]. The results of $A(\omega)$ plotted in Fig. 4 recover nicely the main feature [15] of ΔR shown in Fig. 2. In particular, the agreement of the calculated line shape for the FMR with the measured curve is excellent, which allows us to fit accurately the dimensionless Gilbert damping parameter $\alpha = 0.0075$. Such a good agreement confirms Eq. (1), which demonstrates that the bolometric effect in the FM metal bridges the spin dynamics and the dc charge transport. Based on the model, we conclude that the nonresonant photoresistance is induced by the eddy current dissipation.

The shifted FMAR of the FM grating due to its anisotropic conductivity lies close to dips observed in the photoresistance. However, we note that the discrepancy left in Fig. 3(a) between the dotted curve for the FMAR and open circles for dips is beyond our experimental accuracy. We would like to briefly point out two theoretical aspects that worth further clarifying. One is the influence of geometric details which are neglected in our macroscopic conductivity approximation. They may be analyzed by using an exact calculation as has been nicely discussed by Camley *et al.* [16]. The other effect is the exchange field that is neglected in our model, which can induce spin waves [5]

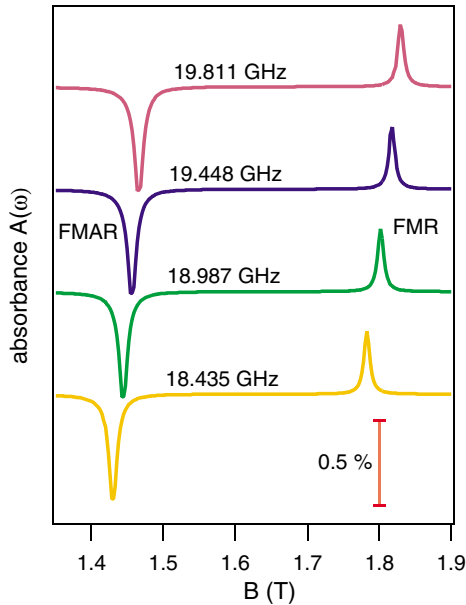


FIG. 4 (color online). The microwave absorbance of the Py grating calculated for different microwave frequencies. The curves are vertically offset for clarity.

and change the behavior of microwave propagation in FM [17]. Nevertheless, our simple model demonstrates the dynamic mixing of spin and charge effect via the interplay of the FMR and the eddy current dissipation. In the same physical sense, but mathematically more sophisticated, one might study the interplay of spin waves and the eddy current response, to examine the role of the exchange field played in the resonant dip observed in our experiment.

We summarize our work from both a technical and physical point of view. The technical difference between the photoconductivity and transmission experiment is obvious. While a transmission experiment measures $A(\omega)$ in Eq. (1) (or equivalently, the *high frequency surface impedance*) by monitoring the absorption of photons, the photoconductivity experiment probes ΔR via the change of the *dc resistance* of spin/charges. The parameter S bridges both and opens free room to enhance the sensitivity. The photoconductivity technique provides a new alternative means to investigate spin excitations in micro and nanomagnets, which used to be measured by either microwave transmission [5,6] or Brillouin light scattering spectroscopy [18]. In principle, the photoconductivity technique can probe the spin dissipation via α , as well as the energy dissipation via τ_e ; both are currently of great interest for investigating magnetodynamics.

From the physical point of view, we developed a macroscopic model that fits excellently well with both the resonant peak and the nonresonant background of the measured photoresistance, which we identify as being caused by microwave power dissipations via the FMR and the eddy current, respectively. Our model reveals also the interplay between the FMR and the eddy current response, which results in a characteristic shift of FMAR in a FM grating by

its anisotropic conductivity. The shifted FMAR locates close to the resonant dips we found in the photoresistance. The physical effect of the dynamic mixing of spin and charge responses, together with the photoconductivity technique that bridges magnetostatics and magnetodynamics, could pave the way for integrating electronic, spintronic, and photonic effects using FM microstructures.

This work is partially supported by the EU 6th-Framework Programme through Project No. BMR-505282, the DFG through SFB 508, and BMBF through Project No. 01BM905. We thank D. Heitmann, F. Giessen, D. Grundler, H.P. Oepen, and R.E. Camley for discussions, D. Görlitz, G. Meier, R. Bose, and J. Becker for technical helps.

*Electronic address: hu@physnet.uni-hamburg.de

- [1] M. Tsoi *et al.*, Nature (London) **406**, 46 (2000).
- [2] S.I. Kiselev *et al.*, Nature (London) **425**, 380 (2003); W.H. Rippard *et al.*, Phys. Rev. Lett. **92**, 027201 (2004).
- [3] C.-M. Hu *et al.*, Phys. Rev. B **67**, 201302(R) (2003); S. Holland *et al.*, Phys. Rev. Lett. **93**, 186804 (2004).
- [4] F. Neppel *et al.*, Phys. Rev. B **19**, 5240 (1979); K. Hirakawa *et al.*, Phys. Rev. B **63**, 085320 (2001); C. Zehnder *et al.*, Europhys. Lett. **63**, 576 (2003).
- [5] C. Kittel *Introduction to Solid State Physics* (John Wiley & Sons, Inc., New York, 1986) 6th ed.
- [6] W.A. Yager, Phys. Rev. **75**, 316 (1949); J.F. Cochran and B. Heinrich, IEEE Trans. Magn. **16**, 660 (1980); A. Schwartz *et al.*, cond-mat/0010172.
- [7] Because of the remanence of the superconducting coil of our magnet, a magnetic-field offset of -1.5 mT has been corrected in the plot.
- [8] A.O. Adeyeye *et al.*, J. Appl. Phys. **79**, 6120 (1996); M. Steiner *et al.*, J. Appl. Phys. **95**, 6759 (2004).
- [9] A. Hubert and R. Schaefer, *Magnetic Domains—The Analysis of Magnetic Microstructures* (Springer-Verlag, Berlin, 1998).
- [10] J.D. Jackson, *Classical Electrodynamics* (John Wiley & Sons, New York, 1998) 3rd ed.
- [11] J.P. Nibarger *et al.*, Appl. Phys. Lett. **83**, 93 (2003).
- [12] M. Nevière, in *Electromagnetic Theory of Gratings*, edited by R. Petit, Springer Topics in Modern Physics Vol. 22 (Springer-Verlag, Heidelberg, 1980).
- [13] Lian Zheng *et al.*, Phys. Rev. B **41**, 8493 (1990).
- [14] K. Bittkau *et al.*, Phys. Rev. B **71**, 035337 (2005).
- [15] To reproduce the measured amplitude for the dips, we have phenomenologically assumed a small energy loss ($< 1\%$) for reflections at the FM/GaAs interface in our calculation, which is not yet clear whether it may reflect the influence of the surface leaky wave of the grating as in the Wood's anomaly (Ref. [12]).
- [16] R.E. Camley *et al.*, Phys. Rev. B **53**, 5481 (1996).
- [17] In a thick sample with $d = 230$ nm, we are able to detect a series of peaks of standing spin waves, while the resonant dip is shifted.
- [18] C. Mathieu *et al.*, Phys. Rev. Lett. **81**, 3968 (1998); Z. K. Wang *et al.*, Phys. Rev. Lett. **89**, 027201 (2002); K. Perzlmaier *et al.*, Phys. Rev. Lett. **94**, 057202 (2005).